

## Induction of Heparanase in Bovine Granulosa Cells by Luteinizing Hormone: Possible Role during the Ovulatory Process

Eyal Klipper, Ehud Tatz, Tatiana Kisiouk, Israel Vlodavsky, Uzi Moallem, Dieter Schams, Yaniv Lavon, David Wolfenson, and Rina Meidan

Department of Animal Sciences (E.K., E.T., T.K., Y.L., D.W., R.M.), Faculty of Agriculture, Food, and Environment, The Hebrew University of Jerusalem, Rehovot 76100, Israel; Cancer and Vascular Biology Research Center (I.V.), The Bruce Rappaport Faculty of Medicine, Technion, Haifa 31096, Israel; Department of Dairy Cattle (U.M.), Institute of Animal Sciences, Volcani Center, Bet-Dagan 50250, Israel; and Institute of Physiology (D.S.), Weihenstephan, Technical University of Munich, 85350 Freising-Weihenstephan, Germany

Follicular development, follicular rupture, and corpus luteum (CL) formation are accompanied by extensive tissue remodeling. We examined whether heparanase (HPSE), which cleaves heparan sulfate glycosaminoglycans, is induced during these processes. Prostaglandin F<sub>2</sub> $\alpha$  injection, which initiated luteolysis and the development of a preovulatory follicle, moderately increased *HPSE* mRNA in bovine granulosa cells (GCs). GnRH, used to induce gonadotropin surge, markedly augmented *HPSE* mRNA levels 12 h after its injection. The temporal pattern of *HPSE* gene expression in follicular-luteal transition was further examined in follicles collected before, and 4, 10, 20, 25, and 60 h after GnRH injection. *HPSE* mRNA increased transiently 10–20 h after GnRH injection to levels 10-fold higher than in untreated heifers. HPSE protein levels were similarly elevated 20 h after GnRH injection in GCs, but not in the theca layer. Cyclooxygenase-2 (*PTGS2*) mRNA peaked before ovulation when *HPSE* levels returned to baseline levels. *HPSE* mRNA abundance also remained low in the CLs. The antiprogesterone, RU-486, elevated *HPSE* levels in GC culture, suggesting that progesterone secreted by CLs may inhibit *HPSE*. HPSE immunostaining was more abundant in GCs than thecae. In cultured GCs, LH induced a transient increase in *HPSE* mRNA 3–6 h after its addition, but not at 24 h. However, *PTGS2* mRNA was clearly induced at this time. These findings suggest that: 1) HPSE may play a role in ovulation but much less so during CL development, and 2) GC-derived HSPE may be a novel member of the LH-induced extracellular matrix-degrading enzyme family and may contribute to follicular rupture. (*Endocrinology* 150: 413–421, 2009)

Extensive tissue remodeling occurs during the ovarian cycle; follicular development, follicular rupture, and the formation and regression of the corpus luteum (CL) require continuous changes in composition and/or degradation of the extracellular matrix (ECM) (1–3). The ECM provides mechanical support of tissue and influences numerous cellular processes, including effects on cell shape and behavior, such as migration, cell anchorage, division, and differentiation (4, 5). The major molecular constituents of ECM are collagens, fibronectin, laminin, and heparan sulfate proteoglycan (perlecan, HSPG) (4, 5).

Several different proteases with differing substrate specificities are required for ECM remodeling and degradation. Two proteolytic systems that have been widely implicated in ovarian matrix remodeling during ovulation and subsequent CL development are the plasminogen activator and the matrix metalloproteinase systems (1, 6–8). These systems are composed of proteases and associated inhibitors that tightly control the proteolytic activity in the extracellular space and, thereby, the site and extent of ECM remodeling. Another proteolytic enzyme, a member of a disintegrin and metalloproteinase with thrombospondin-like motifs-1 (ADAMTS-1) family, was recently in-

ISSN Print 0013-7227 ISSN Online 1945-7170

Printed in U.S.A.

Copyright © 2009 by The Endocrine Society

doi: 10.1210/en.2008-0697 Received May 12, 2008. Accepted September 12, 2008.

First Published Online September 25, 2008

Abbreviations: ADAMTS-1, A disintegrin and metalloproteinase with thrombospondin-like motifs-1; CL, corpus luteum; C<sub>T</sub>, threshold cycle number; ECM, extracellular matrix; ER, estrogen receptor; Fl, forskolin and insulin; GC, granulosa cell; HPSE, heparanase; HS, heparan sulfate; HSPG, heparan sulfate proteoglycan; PGF<sub>2</sub> $\alpha$ , prostaglandin F<sub>2</sub> $\alpha$ ; PGR, progesterone receptor; PTGS2, prostaglandin-endoperoxide synthase-2; TC, theca; VEGF, vascular endothelial growth factor.

duced in granulosa cells (GCs) of preovulatory rat follicles after stimulation with LH (9, 10). Quite unexpectedly, the expression of these proteins was found to be species dependent, *e.g.* different members of these proteolytic systems were induced in rats, cattle, and humans, suggesting species differences (1, 7, 9, 11–13).

Heparan sulfate (HS) and HSPGs are important constituents of the ECM and basement membrane. HSPGs, which not only occur in the ECM but are expressed on cell surfaces, are composed of a protein core to which side chains of the complex glycosaminoglycan HS are attached (14). Each HS side chain consists of a linear polysaccharide of up to 400 sugar residues, composed of a repeating disaccharide of hexuronic and D-glucosamine, is substituted to varying extents by O- and N-linked sulfate and N-acetyl groups (15). HSPGs regulate many physiological processes such as adhesion, migration, differentiation, and proliferation (16–18). Furthermore, HS can bind proteins and regulate their availability and function. For example, a number of growth factors bind HS and are sequestered in the ECM and basement membranes (17). In addition, there is clear evidence that cell surface HS can interact with HS-binding growth factors and facilitate signal transduction via growth factor receptors (19).

Heparanase (HPSE) is an endo- $\beta$ -D-glucuronidase that degrades HS glycosaminoglycan side chains of proteoglycans (20, 21). Studies using HPSE overexpressing transgenic mice revealed that this enzyme functions in normal processes involving cell mobilization, HS turnover, and tissue vascularization (22). HSPE appears to be the only endoglycosidase that degrades HS and, thus, is an important participant in ECM solubilization. Therefore, it is likely that HSPE plays a role in ovarian tissue remodeling. Interestingly, inactive HPSE still retained an array of biological functions, suggesting that this molecule has functions that are independent of its enzymatic activity, therefore, increasing its diversity (23). To date, very little information is available regarding HPSE expression and its regulation in ovaries. Here, we examined HPSE expression in the bovine ovary during the periovulatory period and the subsequent luteal phase. To understand better how the HPSE mRNA levels are regulated, we also conducted *in vitro* studies using cultured GCs.

## Materials and Methods

### *In vivo* studies

#### Experiment 1

The estrous cycle of lactating Holstein cows was synchronized by injecting two doses of prostaglandin F<sub>2</sub> $\alpha$  (PGF<sub>2</sub> $\alpha$  analog) (625  $\mu$ g cloprostenol, Estrumate; Coopers, Berkhamsted, UK) administered 12 d apart. Animals were observed for estrous behavior three times a day for 2 d, starting 36 h after the second PGF<sub>2</sub> $\alpha$  injection. Only animals exhibiting overt estrous behavior and with ultrasound-confirmed ovulation (36–48 h after the onset of estrus) were included in the experiment. From d 3 of the succeeding cycle, ultrasonography was performed daily with a real-time ultrasound instrument (model SSD-900; Aloka, Tokyo, Japan) equipped with a 7.5-MHz transrectal linear transducer. Cows were sorted randomly into four experimental groups. On d 6 of the cycle, GCs were aspirated from the first-wave dominant follicles (group 1), or PGF<sub>2</sub> $\alpha$  was injected (to induce luteolysis and development of a preovu-

latory follicle). Preovulatory follicles were aspirated 24 or 42 h later (groups 2 and 3, respectively). A fourth group of cows was injected with GnRH (250  $\mu$ g gonadorelin acetate, Gonabreed; Parnell Laboratories, Alexandria, Australia) 48 h after PGF<sub>2</sub> $\alpha$  injection, and GCs were aspirated 12 h later. For retrieval of GCs (24), cows were injected im with 14 mg xylazine hydrochloride (Sedaxylan; Eurovet Animal Health BV, Bladel, Holland) to induce effacement and muscle relaxation to minimize rectal contractions, and with 2.5 ml (2%) lidocaine for achieving local anesthesia. GCs were collected using a 7.5-MHz intravaginal sectorial ultrasound probe (Pie Medical, Maastricht, The Netherlands), which was attached to a metal rigid pipeline ending with an aspiration-needle (21 gauge), which was then attached to a 5-ml syringe. The pipeline and the attached syringe were filled with sterile saline solution (NaCl 0.9%). The contents of the chosen follicle were aspirated and repumped two to three times to facilitate detachment of the GCs from the follicle wall. After centrifugation (2000 rpm, 5 min), follicular fluids were kept at –20 C, and the cell pellets were subjected to RNA extraction. There were 28 cows included in this experiment.

#### Experiment 2

The experimental procedure was described previously by Berisha *et al.* (25). The animal experiments were approved by the Bavarian Authority Institutional Care (AZ 211-2531.3-33/96) and Use Committee.

FSH (Ovagen, Immunochemical Products Ltd., Auckland, New Zealand) injections (a total of seven) were given im at 12-h intervals in gradually decreasing doses: two times 1.4 mg, two times 1.2 mg, two times 1.1 mg, and a last injection of 1.0 mg FSH. After the sixth FSH injection, a luteolytic dose of 500  $\mu$ g PGF<sub>2</sub> $\alpha$  analog (cloprostenol, Estrumate; BERNA Veterinärprodukte AG, Bern, Switzerland) was injected im, and 40 h after PGF<sub>2</sub> $\alpha$  injection, 100  $\mu$ g GnRH (Receptal; BERNA Veterinärprodukte AG) was injected to induce the LH surge. For confirmation of LH surge, blood samples were collected from the jugular vein. Before GnRH, basal LH concentrations were present in blood plasma (range 0.8–1.0 ng/ml); 3 h after GnRH, the mean LH level (induced LH surge) was 11.50 ng/ml (range 8.5–14.1), and at 12 h, 0.73 ng/ml (range 0.2–1.0). For each time point [0, 4, 10, 20, 25 h (follicles) and 60 h (new CL)] relative to injection of GnRH, the ovaries were collected by transvaginal ovariectomy. For each time point, five cows were ovariectomized, and one follicle from each was used per time point (n = 5 follicles from five different cows per group). The other follicles from superovulated animals were used in other experiments. Only follicles that appeared healthy (*i.e.* well vascularized and having transparent follicular walls and fluid) and whose diameters were more than 10 mm were collected. For RNA extraction, follicles were dissected from the ovary, and the surrounding tissue [theca (TC) externa] was removed with forceps under a stereomicroscope. Follicles were aliquoted, quickly frozen in liquid nitrogen, and stored at –80 C until RNA was extracted.

#### Experiment 3

The estrous cycle of lactating Holstein cows was synchronized as in experiment 1. On d 6 of the estrous cycle, cows were injected with PGF<sub>2</sub> $\alpha$  to induce preovulatory follicular development and were sorted randomly into two experimental groups. One group (n = 4) was injected with GnRH 30 h after the PGF<sub>2</sub> $\alpha$  injection, whereas the other group (n = 4) remained untreated. Ovaries with large follicles (>10 mm in diameter) were collected at a local slaughterhouse 20 h after the GnRH injection. GCs were enzymatically harvested (as described below in *In vitro studies*), after which TC layers were peeled off from the follicle and were immediately frozen. A small fraction of GCs was processed for RNA extraction, and the rest were used for protein determination, as detailed below.

The protocols of experiments 1 and 3 were approved by the local ethics committee of the Hebrew University.

#### CL collection

CLs were collected at a local slaughterhouse, and the luteal stage was determined by macroscopic examination of the ovaries, according to

criteria described by Fields and Fields (26). CLs were divided into three groups: early (d 2–6), mid (d 8–12), and late (d 15–18).

## In vitro studies

### Isolation and culture of GCs

Ovaries with large follicles (>10 mm in diameter) were collected at a local slaughterhouse. To determine the status of the follicles, estradiol and progesterone concentrations were measured in follicular fluid by Diagnostic Products Corp. estradiol and progesterone kits (Diagnostic Products Corp., Los Angeles, CA) according to the manufacturer's instructions. Follicles with estradiol concentrations in follicular fluids more than 100 ng/ml and ratios of estradiol to progesterone more than one were classified as healthy large follicles (27, 28). GCs were enzymatically dispersed (29, 30) using 0.1% hyaluronidase, 0.1% collagenase I, and 5 µg/ml deoxyribonuclease I (Worthington Biochemical Corp., Freehold, NJ). The TC layer was peeled from the ovary. Viability of GCs was examined using Trypan blue staining. TC layers were processed immediately for RNA extraction. GCs ( $0.5\text{--}1 \times 10^6$  cells per well) were seeded in six-well plates and cultured in basal media (DMEM-F12 containing 3% fetal calf serum, 2 mM L-glutamine, and 100 µg/ml penicillin streptomycin; Biological Industries, Kibbutz Beit Hemeek, Israel). Bovine LH (100 ng/ml) or RU 486 (mifepristone, 0.5 µM; Sigma-Aldrich Corp., St. Louis, MO) was added for 3, 6, and 24 h. For *in vitro* luteinization, GCs ( $0.5\text{--}1 \times 10^5$  cells per well) were seeded in 24-well plates and cultured in basal media (described previously) containing forskolin (10 µM; Sigma-Aldrich) and insulin (2 µg/ml; Sigma-Aldrich). Cells were harvested on d 3 and 6 culture (29, 30).

### RNA isolation and real-time PCR

Total RNA was isolated from tissue and cells using Tri-Fast reagent (Peqlab Biotechnologie GmbH, Erlangen, Germany) according to the manufacturer's instructions. PCRs were performed using the PE Biosystems GeneAmp 5700 sequence detection system, with the SYBR Green I PCR kit (Eurogentec, Seraing, Belgium) used as previously described (31, 32). Briefly, each real-time reaction (18 µl) contained the SYBR Green Master Mix that comprised ROX 6-carboxy-X-rhodamine passive reference, 200 µM deoxynucleotide triphosphates, including deoxyuridine 5-triphosphate, 5 mM MgCl<sub>2</sub>, uracil N-glycosylase, and Amplitaq HotGoldStar DNA polymerase, 0.54 µl of a 1:10,000 dilution of SYBR Green stock solution, 1.5 mM deoxynucleotide triphosphates, 10 nM of each primer, and 5–50 ng cDNA. The glyceraldehyde 3-phosphate dehydrogenase gene was used as the housekeeping gene for CL, TC, and GC from follicles. For cultured cells, actin β was used as the housekeeping gene. Dissociation curve analysis was performed after each real-time experiment to confirm the presence of only one product and the absence of the formation of primer dimers. The threshold cycle number (C<sub>t</sub>) for each tested gene X was used to quantify the relative abundance of the gene; arbitrary units were calculated as:  $2^{-\Delta C_t} = 2^{-(C_t \text{ target gene X} - C_t \text{ housekeeping gene})}$ . Table 1 presents a list of primers.

### Western blot analysis

Cell extraction was performed as described by D'Souza *et al.* (33). Briefly, 6–10 × 10<sup>6</sup> GCs were homogenized in lysis buffer [50 mM Tris HCl, 8 M urea, 1% sodium dodecyl sulfate, 1% β-ME (pH 7), and 10% protease inhibitor cocktail]. Cell lysates were sonicated on ice for 10 sec at low speed. Proteins were precipitated overnight at 4 C by 100% (wt/vol) trichloroacetic acid (diluted 1:4 with sample). Protein pellets were washed twice with 500 µl acetone and air-dried. Finally, samples were resuspended in sodium dodecyl sulfate sample buffer containing βME, boiled, and centrifuged before being loaded onto the polyacrylamide gel. Proteins were electrically transferred to nitrocellulose membranes, blocked for 2 h in Tris-buffered saline-Tween 20 containing 5% low-fat milk, then washed and incubated overnight at 4 C with monoclonal human anti-HPSE antibody (InSight Biopharmaceuticals, Rehovot, Israel). The antibody was diluted 1:1000 in 0.5% low-fat milk. Membranes were then washed three times and incubated with horseradish

TABLE 1. Primer list

Gene	Sequences	Product length (bp)
GAPDH	f: ggcgtgaaccacgagaagat r: cgtggacagtgggtcataagt	141
ACTB	f: cgggacctgacggactacct r:gccatctcctgctcg aagtcc	137
CYP19A1	f: tgggtgatgatgaaggctgctc r: cgaggc actgtct gaattct	180
PGR	f: caggc tggc atggtcttgg r: ggc ttaggc ttggc tttcgt	127
HPSE	f: cgattgttgagaagatcaga r: aaggtgttgaca ggaagg	102
VEGF	f: ccatgaactttctg tcttgg r: tccatgaactcacc acttcg	135
PTGS2	f: cagcggtcgacaaatcctt r:ctgtgtgggagt gggttca	179

ACTB, Actin β; f, forward; GAPDH, glyceraldehyde 3-phosphate dehydrogenase; r, reverse.

peroxidase-conjugated goat antimouse IgG for 1 h at room temperature. A chemiluminescent signal was generated with SuperSignal (Thermo Scientific, Rockford, IL), and the membranes were exposed to x-ray film.

### Immunohistochemistry

The procedure was performed as described previously (34, 35). Follicles were fixed in 4% (vol/vol) paraformaldehyde (Sigma-Aldrich), embedded in paraffin, and cut into 5-µm sections. The sections were dewaxed in xylene and rehydrated using decreasing ethanol concentrations. Endogenous peroxidase activity was quenched by pretreatment with 3% (vol/vol) hydrogen peroxide (Sigma-Aldrich) in methanol for 30 min. Antigen retrieval was performed by treating sections for 5 min in a microwave in boiling citrate buffer [Na citrate 10 mM (pH 6.0)]. Tissue sections were then washed in PBS and incubated (1 h) with normal horse serum (10%) that served as a blocking agent for nonspecific binding. Tissue sections were then incubated for 18 h with rabbit polyclonal anti-HPSE antiserum (diluted 1:100). After three washes in PBS, the slides were incubated with Dako antirabbit EnVision-horseradish peroxidase-labeled polymer (DakoCytomation, Carpinteria, CA) for 30 min. After a final PBS wash, the immunoreactive proteins were visualized with AEC 3-amino-9-ethylcarboxal solution and then counterstained with hematoxylin.

### Statistical analyses

Data are presented as means ± SEM. Data were analyzed by either one-way ANOVA or the Student's *t* test. Differences were considered significant at *P* < 0.05. All data were assessed for heterogeneity of variance using a Bartlett test and were found to be nonsignificant.

## Results

### HPSE and aromatase mRNA levels in GCs during follicular development and GnRH administration

In experiment 1, GCs were retrieved from first-wave dominant follicles (d 6 of the cycle) or from preovulatory follicles collected 24 and 42 h after PGF2α injection (Fig. 1). The mRNA levels of cytochrome P450 aromatase (CYP19A1) in GCs and the estradiol concentrations in follicular fluids were used to ascertain the stage of follicular development. CYP19A1 mRNA levels were low before PGF2α was administered but increased progressively after PGF2α was injected, reaching the highest level 42 h after PGF2α (Fig. 1).

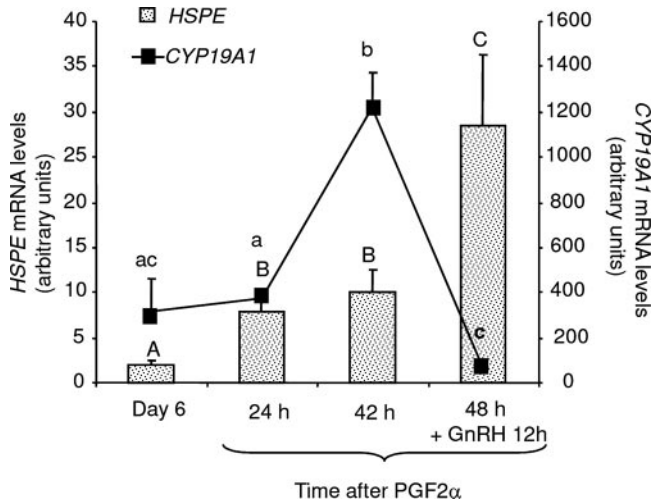


**FIG. 1.** *HPSE* and *CYP19A1* mRNA abundance in GCs during follicular development and GnRH-induced gonadotropin surge (experiment 1). GCs were aspirated from first-wave dominant follicles on d 6 of the cycle and from preovulatory follicles collected 24 and 42 h after PGF2α injection and 12 h after GnRH, administered 48 h after PGF2α injection. RNA was extracted from cells at each time point (n = 5–7 for each group) and reverse transcribed. *HPSE* and *CYP19A1* were determined by real-time PCR. Arbitrary units represent relative gene expression and are calculated as:  $2^{-(Ct_{gene} - Ct_{GPDH})}$ . Results are presented as means ± SEM. No common letters indicate significant differences ( $P < 0.05$ ; uppercase for *HPSE* and lowercase for *CYP19A1*).

*CYP19A1* mRNA correlated well with estradiol concentrations in follicular fluids (data not shown), and both measures confirmed that PGF2α injection promoted follicular development. *HPSE* mRNA levels increased as follicles progressed to become preovulatory follicles. Its levels in GCs increased 3-fold, 24 and 42 h after PGF2α administration, as compared with follicles on d 6 of the cycle (Fig. 1). An additional, significant increment in *HPSE* mRNA occurred 12 h after GnRH was administered to preovulatory follicles (11-fold increase compared with d 6 follicle), suggesting LH-induced increase in the steady-state levels of *HPSE* mRNA. As expected, GnRH sharply reduced *CYP19A1* levels in preparation for ovulation (Fig. 1).

**Temporal gene expression in preovulatory follicles or newly formed CLs after GnRH-induced LH surge**

To resolve more precisely the dynamics of *HPSE* gene expression in preovulatory follicles exposed to the gonadotropin surge, we determined next its levels in whole follicles collected from superovulated heifers (25), 4, 10, 20, 25, and 60 h after GnRH: experiment 2 (Fig. 2). Steady-state *HPSE* mRNA levels exhibited a transient induction profile; it was low before GnRH treatment but increased significantly 10 and 20 h after GnRH (or 7–17 h after the LH surge), to levels approximately 12-fold higher (Fig. 2A). Twenty-five hours after GnRH [~5 h before expected ovulation (25)] and 60 h after GnRH (early CL), *HPSE* returned to basal levels. The mRNA levels of other genes [progesterone receptor (*PGR*) and prostaglandin-endoperoxide synthase-2 (*PTGS2*), also known as cyclooxygenase-2] were also measured in the same samples. The known pattern of these genes (36–38) was used to ascertain the expected temporal profile, and to compare it with that of the *HPSE* gene. All genes exhibited unique temporal expression. *PTGS-2* mRNA levels increased

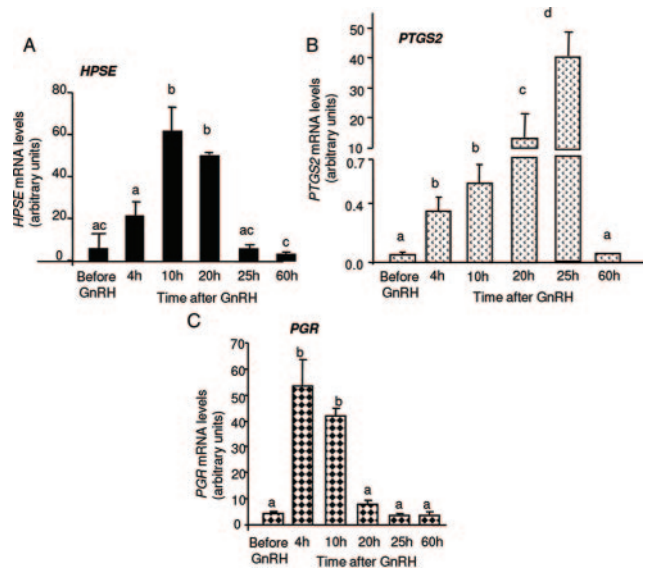


**FIG. 2.** *HPSE* (A), *PGR* (C), and *PTGS2* (B) mRNA levels in preovulatory follicles or newly formed CL collected at 0, 4, 10, 20, and 25 h (follicles), and at 60 h (new CL) after injection of GnRH (experiment 2). RNA was extracted, reverse transcribed, and the cDNA was subjected to real-time PCR. Arbitrary units represent relative gene expression and are calculated as:  $2^{-(Ct_{gene} - Ct_{GPDH})}$ . For each time point, five heifers were ovariotomized, and one follicle of each was taken (n = 5 follicles from five different cows per time point). Results are presented as means ± SEM. No common letters indicate significant differences ( $P < 0.05$ ).

steadily toward the expected time of ovulation, reaching their peak 25 h after GnRH (~22 h after LH surge), 15 h after those of *HPSE*, and became undetectable 60 h after GnRH (early CL; Fig. 2C). *PGR* exhibited a significant change already 4 h after GnRH; in fact, its levels at this time point were already maximal, and declined at 20 and 25 h after GnRH as well as in the young CLs (Fig. 2B).

**HPSE mRNA levels in CLs at different stages of the luteal phase**

Because this last experiment only contained very early CL samples, *HPSE* mRNA levels at different stages of the luteal phase were then determined (Fig. 3). *HPSE* mRNA was low in CLs collected on d 2–6 of the cycle, in fact, its levels in these samples were comparable to those found 60 h after GnRH (Fig. 2A). There was a 3-fold increase in *HPSE* mRNA at midcycle CL,

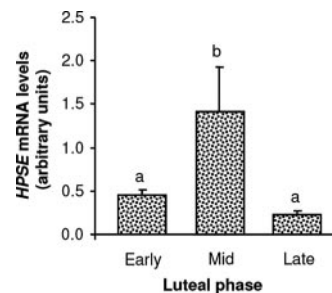


**FIG. 3.** *HPSE* mRNA abundance in CLs collected at different stages of the luteal phase. CLs were either from early (d 2–6; n = 7), mid (d 8–15; n = 10), or late (d 16–18; n = 9) luteal phases. Changes in mRNA levels in the different groups were determined by real-time PCR. Arbitrary units represent relative gene expression and are calculated as:  $2^{-(Ct_{gene} - Ct_{GPDH})}$ . Different letters indicate significant differences ( $P < 0.05$ ).

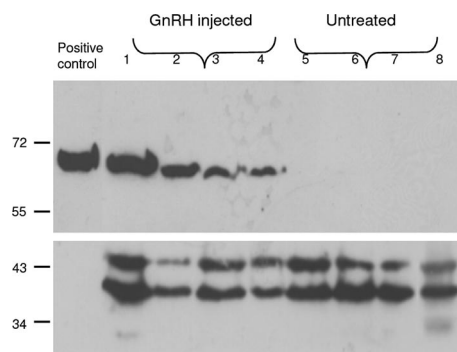


**FIG. 4.** Induction of HPSE protein levels in GCs of bovine preovulatory follicles in response to GnRH (experiment 3). GC protein extracts from untreated cows or at 20 h after GnRH injection were collected and analyzed by Western blotting, as described in *Materials and Methods*. Lanes 1–4 and 5–8 each represent four individual follicles (one per cow) from GnRH-injected or normal preovulatory cows, respectively. Anti-HPSE monoclonal antibody was used to determine the levels of HPSE in these samples. Western blotting of total MAPK was used as a loading control. HPSE overexpressing cell extract was used as a positive control.

followed by a decrease during the late luteal phase (Fig. 3). Nevertheless, HPSE levels in the CLs, even at midcycle, were at least one order of magnitude lower than those present during the periovulatory period (Figs. 2 and 3).

#### Induction of HPSE protein levels in GCs of preovulatory follicles by GnRH

To determine whether the induction of *HPSE* mRNA during the periovulatory period (Fig. 2A) was accompanied by an elevation of its protein levels, we collected follicles 20 h after GnRH injection (experiment 3) and probed GC protein extracts for HPSE using a specific antibody. As shown in Fig. 4, there was indeed a dramatic elevation in HPSE protein levels in GC derived from GnRH-injected cows, as compared with cells from untreated preovulatory follicles. These GCs exhibited the expected increase in *HPSE* mRNA. Interestingly, GnRH injection did not alter *HPSE* mRNA in TCs (data not shown).

#### Differential expression of HPSE in GCs and TCs

GCs differed from TCs also in their basal *HPSE* mRNA levels, which were approximately 2-fold higher than those of TCs (Fig. 5).

The immunohistochemical localization of HPSE at the protein level (Fig. 6) was in good agreement with its mRNA abundance, meaning that the GC layer was more intensely stained than the TC layer in both the small and large follicles. In general, there was a stronger staining in the large (Fig. 6, A and B) *vs.* the small follicles (Fig. 6C).

#### In vitro regulation of HPSE in GCs

GCs were incubated with LH for different time periods ranging from 3–24 h (Fig. 7A). LH up-regulated *HPSE* mRNA levels after 3 and 6 h culture to levels approximately 4-fold higher than controls. Similarly to the *in vivo* results, the stimulatory effect of LH was transient because no increase was observed when cells were incubated with LH for 24 h. To ascertain whether the cells remained responsive at this time point, we probed another LH-dependent gene, *PTGS2*, in these samples as well. As expected,

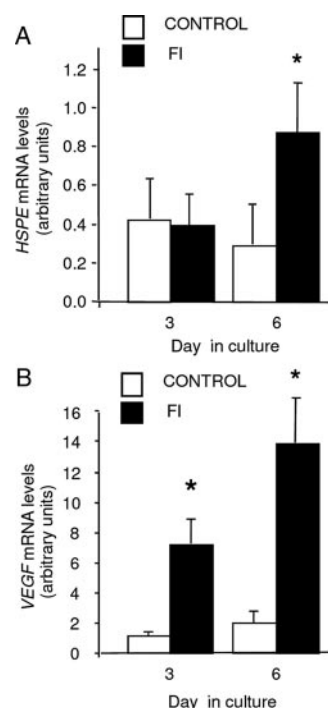


**FIG. 5.** *HPSE* mRNA abundance in granulosa (GC) and TC cell layers from large, healthy follicles. RNA was extracted from GCs and TCs of large follicles ( $n = 12$ ), followed by reverse transcription and real-time PCR analysis. Arbitrary units represent the relative gene expression and are calculated as:  $2^{-CT_{\text{gene}} - CT_{\text{GPDH}}}$ . Results are presented as means  $\pm$  SEM. Different letters indicate significant differences ( $P < 0.05$ ).

LH and FRS stimulated *PTGS2* mRNA at 24 h (Fig. 7B). The effect of the PGR antagonist, RU-486, on *HPSE* gene expression was also examined. This compound elevated *HPSE* mRNA levels, but this effect was only evident 24 h after its addition (Fig. 7C).

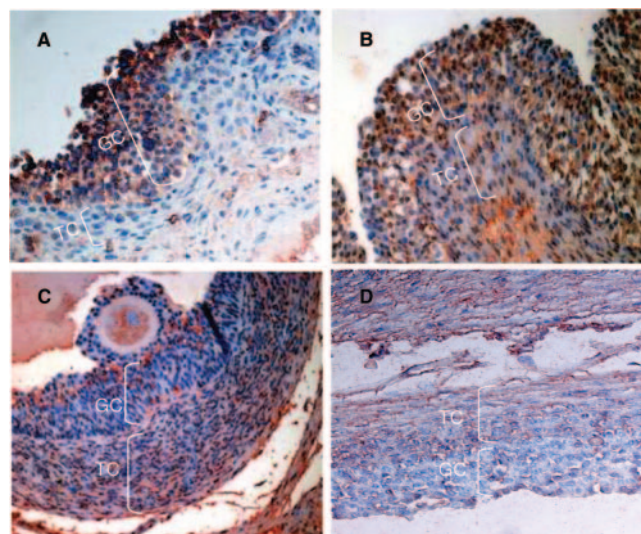


**FIG. 6.** Immunolocalization of HPSE in bovine follicles. Follicles were fixed in 4% (vol/vol) paraformaldehyde, embedded in paraffin, and cut into 5- $\mu$ m sections. Tissue sections were then incubated with rabbit polyclonal anti-HPSE antiserum (Pab 733). A and B, Preovulatory follicles. C, Small antral follicle. D, Negative control. Preovulatory follicle sections were incubated in the presence of nonimmune serum. Positive staining appears in dark red-brown. All sections were counterstained with hematoxylin (blue). A–D were photographed at  $\times 100$  magnification. GC, GC layer; TC, TC cell layer.

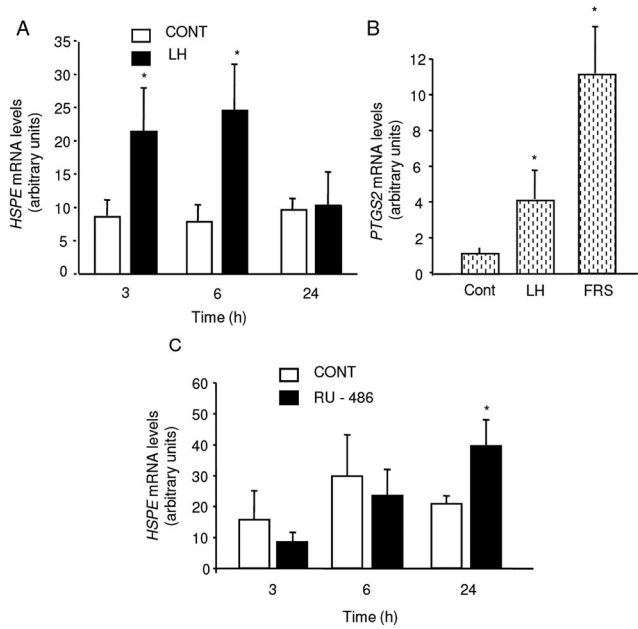


**FIG. 7.** *HPSE* and *PTGS2* mRNA abundance in cultured GCs. GCs were incubated with either LH (100 ng/ml; A) or RU 486 (0.5  $\mu$ M; C) for 3, 6, and 24 h (A and C, *HPSE* mRNA). B, *PTGS2* mRNA abundance; GCs were cultured with LH (100 ng/ml) or FRS (10  $\mu$ M) for 24 h. mRNA levels were measured by real-time PCR. Arbitrary units represent relative gene expression and are calculated as  $2^{-(Ct_{\text{gene}} - Ct_{\text{GPDH}})}$ . Data represent the means  $\pm$  SEM from four independent experiments. \*, Significant ( $P < 0.05$ ) difference in comparison with the matching control time point. CONT, Control.

Next, we examined *HPSE* mRNA levels during *in vitro* luteinization of GCs. Cells were cultured in the presence or absence of forskolin and insulin (FI) (Fig. 8). On d 3, FI treatment did not affect *HPSE*; however, it moderately elevated the *HPSE* level on d 6 culture (Fig. 8A). In contrast, FI induced a marked increase in vascular endothelial growth factor (*VEGF*) mRNA (4- to 5-fold *vs.* control) both on d 3 and 6 culture (Fig. 8B).

### Discussion

The present study demonstrates for the first time that *HPSE* is markedly induced during the ovulatory process. This induction was observed *in vivo*, in GCs and in whole follicles during GnRH-induced gonadotropin surge and in cultured GCs challenged with LH. TCs had lower levels of *HPSE* than GCs, which remained unaffected by GnRH. These results suggest the involvement of GC-derived *HPSE* in LH-induced events during the peri-ovulatory period and possibly in ovulation itself.

Successful ovulation is necessary for fertilization and reproductive success. Coinciding with the termination of specific gene expression in mature follicles, LH induces a set of genes that culminate in ovulation (39, 40). Because the ovulatory process involves follicular rupture, extensive proteolytic degradation of the basement membrane and connective tissue composing the follicular wall takes place (8, 41). Many studies have shown that several protease families, plasminogen activator, matrix metalloproteinase systems, and ADAMTS-1 are induced in GCs by the LH surge, suggesting that it plays a role in degrading the ovarian

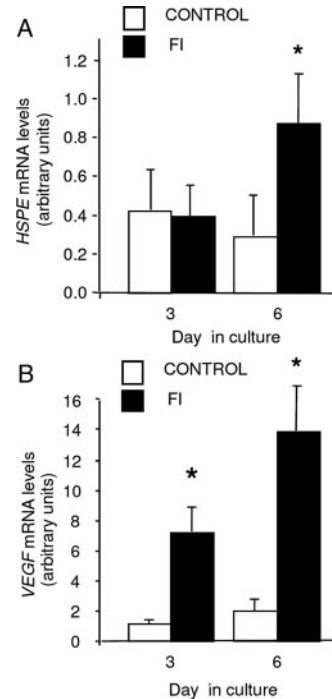


**FIG. 8.** *HPSE* and *VEGF* mRNA abundance in GCs undergoing *in vitro* luteinization. GCs were incubated with forskolin (FRS) (10  $\mu$ M) and insulin (2  $\mu$ g/ml) for 3 and 6 d. *HPSE* (A) and *VEGF* (B) mRNA levels were measured by real-time PCR. Arbitrary units represent relative gene expression and are calculated as  $2^{-(Ct_{\text{gene}} - Ct_{\text{GPDH}})}$ . Data represent means  $\pm$  SEM from three independent experiments. \*, Significant ( $P < 0.05$ ) difference in comparison with the matching control time point.

follicular wall during ovulation (6, 8, 41). The expression pattern of *HPSE* reported here suggests that it may be a novel member of LH-induced ECM-degrading enzymes that participates in follicular rupture in cattle. Its possible involvement in ovulation in other species remains to be determined.

Although the time span of the ovulatory process varies among mammalian species, the cellular mechanisms involved are rather well preserved. Both the *PGR* and *PTGS2* induced by the LH surge (36, 37, 42, 43) were shown, in many species, to be indispensable for ovulation. Their pharmacological inhibition or genetic elimination prevents expulsion of the oocyte, which remains trapped in the follicle. In cattle, the *PGR* is quickly induced by 4 h (~1 h after LH surge), and it remains high for at least 10 h after GnRH administration (Ref. 44 and this study). Here, we found that *HPSE* was induced soon after *PGR* mRNA was induced; it remained high 10–20 h after GnRH, and declined later. *PTGS2*, on the other hand, was delayed compared with these two genes and peaked only 25 h after GnRH (~5 h before the expected ovulation).

Clearly, all three mRNAs had unique transient expression profiles; however, whereas the roles of *PGR* and *PTGS2* in the ovulatory process are well understood, the functional consequences of the unique pattern of *HPSE* mRNA steady-state levels and the early induction of *HPSE* mRNA were not previously investigated. However, it is reasonable to assume that cleavage of HS by *HPSE* could directly contribute to ECM breakdown and remodeling in preparation for ovulation. Changes in *HPSE*

mRNA levels were observed here not only during the ovulatory process but also during development of the preovulatory follicle. The composition of the follicle's ECM is continuously modified during follicular development and ovulation. In a series of studies, Rodgers and colleagues (5, 45) had shown that of the HSPGs, perlecan is up-regulated during early follicular development and is degraded at ovulation. Given the high concentration of perlecan-containing focimatrix in the membrana granulosa before ovulation, it is possible that its degradation by HSPE would release sequestered growth factors. This may be an initial part of a cascade of events leading to the migration and proliferation of cells from the TC interna during formation of the CL.

Degradation of HS in the basement membrane of blood vessels is known to promote angiogenesis (16, 17) by facilitating endothelial cell invasion through the subendothelial basement membrane (19, 46). Furthermore, Hspe gene silencing is associated with a marked reduction in tumor angiogenesis (47). CL formation is one of the few physiological angiogenic events that occur in adults (48, 49). Therefore, it was unexpected to find that *HSPE* expression was down-regulated much before angiogenesis commences in the CLs. Moreover, we showed here that *HSPE* levels in the CLs remain low throughout the luteal phase. In contrast to *HSPE*, VEGF, a *bona fide* angiogenic factor, is up-regulated in CLs soon after ovulation, and remains elevated in the mature and active glands (48, 50). Luteinizing agents (either LH or forskolin) maintained their ability to induce VEGF in GCs *in vitro*. In addition, unlike *HPSE*, *VEGF* expression was not transient but instead exhibited a sustained induction. For both *HSPE* and *VEGF*, the *in vitro* data were highly consistent with the *in vivo* regulation of these genes. In fact, there was a small increase in *HPSE* mRNA both *in vivo* during midcycle, and *in vitro*, but only in cells incubated for 6 d with luteinizing agents and not at earlier time points. The importance of this expression pattern of *HSPE* remains unclear. However, it should be emphasized that *in vivo* as well as *in vitro*, *HPSE* levels were much higher in GCs or whole follicles than in luteal cells or CLs. The lack of significant *HSPE* gene expression in CLs, unlike in tumors, for instance, is intriguing and may suggest a preferential role for the enzyme in cancer *vs.* physiological angiogenesis. This observation may also be related to the fact that *HSPE* was localized to endothelial cells of vessels within invasive cancers (51, 52), whereas it was absent (both mRNA or protein) in luteal endothelial cells (our unpublished data).

*HPSE* may play an additional role during ovulation, which is unrelated to its enzymatic activities. It was recently shown that *HPSE* localizes in the nucleus and contributes to the induction of various genes, and especially *PTGS2* (53). *HSPE* and *PTGS2* expression are highly correlated in cancer cells (54, 55), as well as in cells transfected with *HSPE* cDNA, and up-regulation of *PTGS2* was observed (56). Therefore, it is suggested that *HSPE* could play a role in *PTGS2* induction during the periovulatory period. Several lines of evidence support this proposition: 1) *HSPE* peaks before *PTGS2* during the periovulatory period, 2) both genes are expressed by the same cell type (GC), and 3) both genes are induced in GCs in response to LH. Experiments are now being conducted in our laboratory to elucidate the relationship between *HSPE* and *PTGS2*.

Examination of the transcriptional activation of *HPSE* revealed that its promoter region contains estrogen response elements. Transcription of a reporter gene driven by the *HPSE* promoter was significantly increased in estrogen receptor (ER)-positive MCF-7 human breast carcinoma cells treated with estrogen (57). In another study, it was shown that estrogen augmented *HPSE* expression and HS degradation on the cell surface and in the basement membrane of the endometrium (58). With regard to *HPSE* expression in the ovary (this study and Ref. 52), follicular GCs are not only major estradiol producers; they were also shown to possess ERs [ER  $\beta$  (59)], enabling the autocrine regulation of *HPSE* by estradiol. Yet when *HSPE* peaks (>20 h after GnRH), estradiol levels have already been reduced as a result of LH-induced suppression of *CYP19A1* (60). This argues against the involvement of estradiol in ovarian *HSPE* expression. This is further supported by the *in vitro* data reported here, showing that LH has a direct stimulatory effect on *HPSE* in GCs cultured without a source of aromatizable androgens.

Adding RU-489, a PGR antagonist to cultured GCs, elevated *HSPE* mRNA levels, as compared with untreated cells. Therefore, one may hypothesize that the periovulatory increase in progesterone levels is responsible for the dramatic decrease in mRNA for *HPSE* observed before ovulation. This may be relevant, in addition to the CLs, where progesterone secreted by the developing CLs may inhibit *HPSE*. Nevertheless, the detailed effects and role of progesterone in *HSPE* induction require further research.

In our study, GCs of large bovine antral follicles expressed higher *HPSE* mRNA levels and were more intensely stained with anti-*HSPE* antiserum than TC interna cells. This staining pattern was also observed in small follicles. These findings appear to contradict a previous study in which *HSPE* was immunolocalized primarily in TC interna of follicles but also in both luteal cell types within human and rat CL (61). However, the latter study did not quantify *HSPE* protein or mRNA in follicles *vs.* CLs.

In summary, the findings reported here show that *HSPE* is transiently induced by LH during the ovulatory process and may be down-regulated by the increasing progesterone levels in the CLs, implying that *HSPE* may play a significant role in ovulation but much less so during CL development. Therefore, *HSPE* appears to be a novel member of the LH-induced ECM-degrading enzyme that contributes, together with other proteases, to follicular rupture. *HPSE* may also affect ovulation by participating in *PTGS2* expression. Future studies targeting *HSPE* in follicles will be required to better define its role during ovulation.

## Acknowledgments

Address all correspondence and requests for reprints to: Rina Meidan, Department of Animal Sciences, Faculty of Agricultural, Food and Environmental Quality Sciences, The Hebrew University of Jerusalem, Rehovot 76100, Israel. E-mail: rina.meidan@huji.ac.il.

Disclosure Statement: The authors have nothing to declare.

## References

- Curry Jr TE, Smith MF 2006 Impact of extracellular matrix remodeling on ovulation and the folliculo-luteal transition. *Semin Reprod Med* 24:228–241
- Smith MF, Ricke WA, Bakke LJ, Dow MP, Smith GW 2002 Ovarian tissue remodeling: role of matrix metalloproteinases and their inhibitors. *Mol Cell Endocrinol* 191:45–56
- Irving-Rodgers HF, Rodgers RJ 2005 Extracellular matrix in ovarian follicular development and disease. *Cell Tissue Res* 322:89–98
- Hay E 1991 *Cell biology of extracellular matrix*. 2nd ed. New York: Plenum Press
- Rodgers RJ, Irving-Rodgers HF, Russell DL 2003 Extracellular matrix of the developing ovarian follicle. *Reproduction* 126:415–424
- Ny T, Wahlberg P, Brandstrom IJ 2002 Matrix remodeling in the ovary: regulation and functional role of the plasminogen activator and matrix metalloproteinase systems. *Mol Cell Endocrinol* 187:29–38
- Dow MP, Bakke LJ, Cassar CA, Peters MW, Pursley JR, Smith GW 2002 Gonadotropin surge-induced up-regulation of the plasminogen activators (tissue plasminogen activator and urokinase plasminogen activator) and the urokinase plasminogen activator receptor within bovine periovulatory follicular and luteal tissue. *Biol Reprod* 66:1413–1421
- Smith MF, McIntush EW, Ricke WA, Kojima FN, Smith GW 1999 Regulation of ovarian extracellular matrix remodeling by metalloproteinases and their tissue inhibitors: effects on follicular development, ovulation and luteal function. *J Reprod Fertil Suppl* 54:367–381
- Espey LL, Yoshioka S, Russell DL, Robker RL, Fujii S, Richards JS 2000 Ovarian expression of a disintegrin and metalloproteinase with thrombospondin motifs during ovulation in the gonadotropin-primed immature rat. *Biol Reprod* 62:1090–1095
- Shozu M, Minami N, Yokoyama H, Inoue M, Kurihara H, Matsushima K, Kuno K 2005 ADAMTS-1 is involved in normal follicular development, ovulatory process and organization of the medullary vascular network in the ovary. *J Mol Endocrinol* 35:343–355
- Boerboom D, Russell DL, Richards JS, Sirois J 2003 Regulation of transcripts encoding ADAMTS-1 (a disintegrin and metalloproteinase with thrombospondin-like motifs-1) and progesterone receptor by human chorionic gonadotropin in equine preovulatory follicles. *J Mol Endocrinol* 31:473–485
- Dow MP, Bakke LJ, Cassar CA, Peters MW, Pursley JR, Smith GW 2002 Gonadotrophin surge-induced upregulation of mRNA for plasminogen activator inhibitors 1 and 2 within bovine periovulatory follicular and luteal tissue. *Reproduction* 123:711–719
- Madan P, Bridges PJ, Komar CM, Beristain AG, Rajamahendran R, Fortune JE, MacCalman CD 2003 Expression of messenger RNA for ADAMTS subtypes changes in the periovulatory follicle after the gonadotropin surge and during luteal development and regression in cattle. *Biol Reprod* 69:1506–1514
- Murdoch AD, Dodge GR, Cohen I, Tuan RS, Iozzo RV 1992 Primary structure of the human heparan sulfate proteoglycan from basement membrane (HSPG2/perlecan). A chimeric molecule with multiple domains homologous to the low density lipoprotein receptor, laminin, neural cell adhesion molecules, and epidermal growth factor. *J Biol Chem* 267:8544–8557
- Stringer SE, Gallagher JT 1997 Heparan sulphate. *Int J Biochem Cell Biol* 29:709–714
- Knox SM, Whitelock JM 2006 Perlecan: how does one molecule do so many things? *Cell Mol Life Sci* 63:2435–2445
- Stringer SE 2006 The role of heparan sulphate proteoglycans in angiogenesis. *Biochem Soc Trans* 34:451–453
- Lopes CC, Dietrich CP, Nader HB 2006 Specific structural features of syndecans and heparan sulfate chains are needed for cell signaling. *Braz J Med Biol Res* 39:157–167
- Vlodavsky I, Goldshmidt O, Zcharia E, Atzmon R, Rangini-Guatta Z, Elkin M, Peretz T, Friedmann Y 2002 Mammalian heparanase: involvement in cancer metastasis, angiogenesis and normal development. *Semin Cancer Biol* 12:121–129
- Hulett MD, Freeman C, Hamdorf BJ, Baker RT, Harris MJ, Parish CR 1999 Cloning of mammalian heparanase, an important enzyme in tumor invasion and metastasis. *Nat Med* 5:803–809
- Vlodavsky I, Friedmann Y, Elkin M, Aingorn H, Atzmon R, Ishai-Michaeli R, Bitan M, Pappo O, Peretz T, Michal I, Spector L, Pecker I 1999 Mammalian heparanase: gene cloning, expression and function in tumor progression and metastasis. *Nat Med* 5:793–802
- Zcharia E, Metzger S, Chajek-Shaul T, Aingorn H, Elkin M, Friedmann Y, Weinstein T, Li JP, Lindahl U, Vlodavsky I 2004 Transgenic expression of mammalian heparanase uncovers physiological functions of heparan sulfate in tissue morphogenesis, vascularization, and feeding behavior. *FASEB J* 18:252–263
- Zetser A, Bashenko Y, Miao HQ, Vlodavsky I, Ilan N 2003 Heparanase affects adhesive and tumorigenic potential of human glioma cells. *Cancer Res* 63:7733–7741
- Roth Z, Arav A, Bor A, Zeron Y, Braw-Tal R, Wolfenson D 2001 Improvement of quality of oocytes collected in the autumn by enhanced removal of impaired follicles from previously heat-stressed cows. *Reproduction* 122:737–744
- Berisha B, Steffl M, Amselgruber W, Schams D 2006 Changes in fibroblast growth factor 2 and its receptors in bovine follicles before and after GnRH application and after ovulation. *Reproduction* 131:319–329
- Fields MJ, Fields PA 1996 Morphological characteristics of the bovine corpus luteum during the estrous cycle and pregnancy. *Theriogenology* 45:1295–1325
- Fortune JE 1994 Ovarian follicular growth and development in mammals. *Biol Reprod* 50:225–232
- Ireland JJ, Roche JF 1983 Development of nonovulatory antral follicles in heifers: changes in steroids in follicular fluid and receptors for gonadotropins. *Endocrinology* 112:150–156
- Aflalo L, Meidan R 1993 The hormonal regulation of cholesterol side-chain cleavage cytochrome P450, adrenodoxin, and their messenger ribonucleic acid expression in bovine small-like and large-like luteal cells: relationship with progesterone production. *Endocrinology* 132:410–416
- Meidan R, Girsh E, Blum O, Aberdam E 1990 In vitro differentiation of bovine theca and granulosa cells into small and large luteal-like cells: morphological and functional characteristics. *Biol Reprod* 43:913–921
- Klipper E, Gilboa T, Levy N, Kislouk T, Spanel-Borowski K, Meidan R 2004 Characterization of endothelin-1 and nitric oxide generating systems in corpus luteum-derived endothelial cells. *Reproduction* 128:463–473
- Kislouk T, Podlovni H, Spanel-Borowski K, Ovadia O, Zhou QY, Meidan R 2005 Prokineticins (endocrine gland-derived vascular endothelial growth factor and BV8) in the bovine ovary: expression and role as mitogens and survival factors for corpus luteum-derived endothelial cells. *Endocrinology* 146:3950–3958
- D'Souza SS, Fazleabas AT, Banerjee P, Sherwin JR, Sharkey AM, Farach-Carson MC, Carson DD 2008 Decidual heparanase activity is increased during pregnancy in the baboon (*Papio anubis*) and in vitro decidualization of human stromal cells. *Biol Reprod* 78:316–323
- Kislouk T, Friedman A, Klipper E, Zhou QY, Schams D, Alfaidy N, Meidan R 2007 Expression pattern of prokineticin 1 and its receptors in bovine ovaries during the estrous cycle: involvement in corpus luteum regression and follicular atresia. *Biol Reprod* 76:749–758
- Podlovni H, Ovadia O, Kislouk T, Klipper E, Zhou QY, Friedman A, Alfaidy N, Meidan R 2006 Differential expression of prokineticin receptors by endothelial cells derived from different vascular beds: a physiological basis for distinct endothelial function. *Cell Physiol Biochem* 18:315–326
- Sirois J 1994 Induction of prostaglandin endoperoxide synthase-2 by human chorionic gonadotropin in bovine preovulatory follicles *in vivo*. *Endocrinology* 135:841–848
- Bridges PJ, Komar CM, Fortune JE 2006 Gonadotropin-induced expression of messenger ribonucleic acid for cyclooxygenase-2 and production of prostaglandins E and F $\alpha$  in bovine preovulatory follicles are regulated by the progesterone receptor. *Endocrinology* 147:4713–4722
- Cassar CA, Dow MP, Pursley JR, Smith GW 2002 Effect of the preovulatory LH surge on bovine follicular progesterone receptor mRNA expression. *Domest Anim Endocrinol* 22:179–187
- Richards JS, Russell DL, Ochsner S, Espey LL 2002 Ovulation: new dimensions and new regulators of the inflammatory-like response. *Annu Rev Physiol* 64:69–92
- Acosta TJ, Ozawa T, Kobayashi S, Hayashi K, Ohtani M, Kraetzl WD, Sato K, Schams D, Miyamoto A 2000 Periovulatory changes in the local release of vasoactive peptides, prostaglandin f(2 $\alpha$ ), and steroid hormones from bovine mature follicles *in vivo*. *Biol Reprod* 63:1253–1261
- Ohnishi J, Ohnishi E, Shibuya H, Takahashi T 2005 Functions for proteinases in the ovulatory process. *Biochim Biophys Acta* 1751:95–109
- Sirois J, Sayasith K, Brown KA, Stock AE, Bouchard N, Dore M 2004 Cyclooxygenase-2 and its role in ovulation: a 2004 account. *Hum Reprod Update* 10:373–385
- Robker RL, Russell DL, Espey LL, Lydon JP, O'Malley BW, Richards JS 2000 Progesterone-regulated genes in the ovulation process: ADAMTS-1 and cathepsin L proteases. *Proc Natl Acad Sci USA* 97:4689–4694
- Jo M, Komar CM, Fortune JE 2002 Gonadotropin surge induces two separate increases in messenger RNA for progesterone receptor in bovine preovulatory follicles. *Biol Reprod* 67:1981–1988
- Irving-Rodgers HF, Catanzariti KD, Aspden WJ, D'Occhio MJ, Rodgers RJ

- 2006 Remodeling of extracellular matrix at ovulation of the bovine ovarian follicle. *Mol Reprod Dev* 73:1292–1302
46. Watanabe M, Aoki Y, Kase H, Tanaka K 2003 Heparanase expression and angiogenesis in endometrial cancer. *Gynecol Obstet Invest* 56:77–82
  47. Edovitsky E, Elkin M, Zcharia E, Peretz T, Vlodavsky I 2004 Heparanase gene silencing, tumor invasiveness, angiogenesis, and metastasis. *J Natl Cancer Inst* 96:1219–1230
  48. Fraser HM, Duncan WC 2005 Vascular morphogenesis in the primate ovary. *Angiogenesis* 8:101–116
  49. Reynolds LP, Grazul-Bilska AT, Redmer DA 2000 Angiogenesis in the corpus luteum. *Endocrine* 12:1–9
  50. Berisha B, Schams D, Kosmann M, Amselgruber W, Einspanier R 2000 Expression and tissue concentration of vascular endothelial growth factor, its receptors, and localization in the bovine corpus luteum during estrous cycle and pregnancy. *Biol Reprod* 63:1106–1114
  51. Mikami S, Ohashi K, Katsube K, Nemoto T, Nakajima M, Okada Y 2004 Coexpression of heparanase, basic fibroblast growth factor and vascular endothelial growth factor in human esophageal carcinomas. *Pathol Int* 54:556–563
  52. Haimov-Kochman R, Friedmann Y, Prus D, Goldman-Wohl DS, Greenfield C, Anteby EY, Aviv A, Vlodavsky I, Yagel S 2002 Localization of heparanase in normal and pathological human placenta. *Mol Hum Reprod* 8:566–573
  53. Naomoto Y, Gunduz M, Takaoka M, Okawa T, Gunduz E, Nobuhisa T, Kobayashi M, Shirakawa Y, Yamatsuji T, Sonoda R, Matsuoka J, Tanaka N 2007 Heparanase promotes angiogenesis through Cox-2 and HIF1 $\alpha$ . *Med Hypotheses* 68:162–165
  54. Ohtawa Y, Naomoto Y, Shirakawa Y, Takaoka M, Murata T, Sonoda R, Sakurama K, Yamatsuji T, Gunduz M, Tsujigiwa H, Nagatsuka H, Terada N, Itano S, Horiki S, Yanagihara K, Nakajima M, Tanaka N 2006 The close relationship between heparanase and cyclooxygenase-2 expressions in signet-ring cell carcinoma of the stomach. *Hum Pathol* 37:1145–1152
  55. Imada T, Matsuoka J, Nobuhisa T, Okawa T, Murata T, Tabuchi Y, Shirakawa Y, Ohara N, Gunduz M, Nagatsuka H, Umeoka T, Yamamoto Y, Nakajima M, Tanaka N, Naomoto Y 2006 COX-2 induction by heparanase in the progression of breast cancer. *Int J Mol Med* 17:221–228
  56. Okawa T, Naomoto Y, Nobuhisa T, Takaoka M, Motoki T, Shirakawa Y, Yamatsuji T, Inoue H, Ouchida M, Gunduz M, Nakajima M, Tanaka N 2005 Heparanase is involved in angiogenesis in esophageal cancer through induction of cyclooxygenase-2. *Clin Cancer Res* 11:7995–8005
  57. Elkin M, Cohen I, Zcharia E, Orgel A, Guatta-Rangini Z, Peretz T, Vlodavsky I, Kleinman HK 2003 Regulation of heparanase gene expression by estrogen in breast cancer. *Cancer Res* 63:8821–8826
  58. Xu X, Ding J, Rao G, Shen J, Prinz RA, Rana N, Dmowski WP 2007 Estradiol induces heparanase-1 expression and heparan sulphate proteoglycan degradation in human endometrium. *Hum Reprod* 22:927–937
  59. Schams D, Kohlenberg S, Amselgruber W, Berisha B, Pfaffl MW, Sinowatz F 2003 Expression and localisation of oestrogen and progesterone receptors in the bovine mammary gland during development, function and involution. *J Endocrinol* 177:305–317
  60. Komar CM, Berndtson AK, Evans AC, Fortune JE 2001 Decline in circulating estradiol during the periovulatory period is correlated with decreases in estradiol and androgen, and in messenger RNA for p450 aromatase and p450 17 $\alpha$ -hydroxylase, in bovine preovulatory follicles. *Biol Reprod* 64:1797–1805
  61. Haimov-Kochman R, Prus D, Zcharia E, Goldman-Wohl DS, Natanson-Yaron S, Greenfield C, Anteby EY, Reich R, Orly J, Tsafrii A, Hurwitz A, Vlodavsky I, Yagel S 2005 Spatiotemporal expression of heparanase during human and rodent ovarian folliculogenesis. *Biol Reprod* 73:20–28